Generation of very high-frequency waves by up-conversion in a plasma-loaded free-electron laser

V. Petrillo and C. Maroli
Dipartimento di Fisica, Istituto Nazionale di Fisica Nucleare and Istituto Nazionale di Fisica della Materia, Università di Milano, Via Celoria 16, 20133 Milano, Italy
(Received 14 April 2000)

A free-electron laser loaded with a plasma is able to resonate at two different frequencies. The two waves are copropagating, one with positive slippage while the other has negative slippage. We deduce the nonlinear partial differential equations describing the interaction between the two waves in the slowly-varying-envelope approximation. By injecting a signal at the low frequency, a strong signal is produced at the harmonically related high frequency, with a lethargy time much smaller than that of the spontaneous vacuum emission. This effect could be applied in the generation of very short wavelength radiation, up to the range of hard x rays.

PACS number(s): 41.60.Cr, 41.75.Lx, 52.75.Di

The possibility of generating high-frequency radiation by means of the mechanism of energy conversion between the two resonant frequencies of a free-electron laser (FEL) has been described theoretically by Piovella *et al.* [1] and Sternbach and Ghalila [2], and further demonstrated experimentally by Liu and Marshall [3] and by Levefre *et al.* [4]. In these works a wave guide FEL has been studied. The electron beam is bunched by the low-frequency resonant wave which is injected at high power level from the outside and gives origin to the wave growth at the harmonically related upper resonant frequency.

The two frequencies are described by the formula

$$\omega_{1,2}=\frac{\omega_s}{1+\beta_\parallel}[1\pm\beta_\parallel\sqrt{1-X}], \tag{1}$$

where $\omega_s=c\beta_\parallel k_w/(1-\beta_\parallel)$, $k_w=2\pi/\lambda_w$ is the wave vector of the wiggler magnetic field, $\beta_\parallel=v_\parallel/c$ where $v_\parallel$ is the initial parallel velocity of the beam, the parameter X (<1) is related to the cutoff frequency and transverse dimension b of the wave guide as $X=(\beta_\parallel\gamma_\parallel k_w b)^{-2}$ and $\gamma_\parallel=1/(1-\beta_\parallel^2)^{1/2}$. The regime considered was that where $X>1/\gamma_\parallel^2$, when both waves are forward waves, one with positive and one with negative slippage.

We define the ratio between the resonant frequencies as $\alpha=\omega_1/\omega_2>1$. The previous works [1,2], which were limited to rather small values of α, have shown that the efficiency of the conversion process is particularly large when α is an integer but decreases with increasing α, roughly as $1/\sqrt{\alpha}$. When $X\ll 1$, the ratio α can be approximated as $\alpha\approx 4\gamma_\parallel^2/(1+\gamma_\parallel^2 X)$, while the corresponding estimate for ω_2 is given by $\omega_2\approx\omega_s\beta_\parallel X/(1+\beta_\parallel)$. In the case of the waveguide FEL, the two preceding formulas become, respectively, $\alpha\approx 4\beta_\parallel^2\gamma_\parallel^2 k_w^2 b^2/(1+\beta_\parallel^2 k_w^2 b^2)$ and $\omega_2\approx c/(k_w b^2)$.

The main interest of this scheme lies in the possibility it offers of obtaining, by frequency up-conversion, a radiation with a very short wavelength. Since $\omega_1=\alpha\omega_2$, one can produce a significant amount of power at a very large frequency ω_1 either by increasing the lower frequency ω_2 and/or increasing α. The increase in α may be achieved by enhancing the initial energy of the beam, but the consequence is the contemporary diminution of the process efficiency. It seems then more convenient to increase the low frequency $\omega_2\approx c/(k_w b^2)$, but the dependence of ω_2 on the parameters is not favorable, in this case, because both dimension of the waveguide b and wiggler period λ_w are, in practice, quantities with a very limited range of variation. The process of up-conversion in a waveguide FEL seems, therefore, to be confined to the production of waves in the range of microwaves or, at most, in the range of UVA, but it seems quite impossible to apply it to shorter wavelengths, e.g., the regime of x rays.

In this paper, we propose a way of controlling the dispersion and slippage of the two resonant waves in the FEL that does not present the limitation described above. In this scheme, the control is obtained by filling the wiggler cavity with a plasma, instead of using a waveguide. We will demonstrate that all previous formulas continue to hold simply by rewriting the parameter X as $X=\omega_p^2/(c^2 k_w^2\beta_\parallel^2\gamma_\parallel^2)$, where $\omega_p=(4\pi n_0 e^2/m)^{1/2}$ is the plasma frequency of the electrons of the plasma background with undisturbed density n_0. For instance, with $n_0=4.4\times 10^{16}$ cm^{-3} (plasma frequency $\omega_p=1.18\times 10^{13}$ rad/sec), a wiggler with wavelength $\lambda_w=1$ cm, a beam with the injection value of the Lorentz factor $\gamma_0=406.8$ ($\gamma_\parallel\approx 317$) and a volume density $n_b=5.11\times 10^{14}$ cm^{-3}, we obtain $X=0.039$, a factor $\alpha=100$, a low-frequency wave with wavelength $\lambda_2=5\,\mu$m, and a high-frequency wave with $\lambda_1=50$ nm. As a second example in the x-ray region, with $n_0=1.24\times 10^{17}$ cm^{-3} ($\omega_p=1.98\times 10^{13}$ rad/sec), $\lambda_w=3$ cm, $\gamma_0=28\,700$ ($\gamma_\parallel\approx 10\,000$), $n_b=1.76\times 10^{15}$ cm^{-3}, $X=10^{-3}$, $\alpha=4000$, by injecting a wavelength $\lambda_2=0.6\,\mu$m, one can obtain the high frequency wave with $\lambda_1=1.5$ Å.

The advantage of this new scheme is that X can be strongly increased with respect to the waveguide case, decreasing the ratio α between the two resonant frequencies, if $\gamma_\parallel$ is kept fixed. One can then reach high values of ω_1 without increasing α too much. We will give some considerations on how this parameter, also in the present case, is related to the efficiency of the process. In addition, we think that the present scheme has all the advantages of the up-frequency conversion with respect to the usual harmonic approach [5], namely, (i) the linewidth of the resonant high frequency is larger than that of the low-frequency wave, as opposed to the

harmonic case, leading, in particular, to a smaller energy spread [6], and (ii) the slippage of the high-frequency wave is lower by a factor of α than that of the low-frequency wave (in the harmonic approach the slippage is essentially the same for all harmonics), thus allowing a higher bunching at the short wavelength.

We assume the usual wave equation for the transverse component of the electric field in one dimension, i.e.,

$$\left[\frac{\partial^2}{\partial t^2}-c^2\frac{\partial^2}{\partial z^2}\right]\mathbf{E}_\perp(z,t)=-4\pi\frac{\partial \mathbf{J}_\perp}{\partial t}. \tag{2}$$

$\mathbf{J}_\perp$ is the transverse component of the total current $\mathbf{J}=\mathbf{J}_b+\mathbf{J}_p$ with $\mathbf{J}_p=-en_p\mathbf{u}_p$, and $\mathbf{J}_b=-en_{\perp b}\Sigma_{s=1}^{N_T}\mathbf{v}_s(t)\delta(z-z_s(t))$, where n_p and $\mathbf{u}_p$ are, respectively, the volume density and average velocity of the electrons of the plasma, while $\mathbf{J}_b$ gives the beam current in the charged sheet model ($n_{\perp b}$ is the surface density of the electrons on the single sheet, N_T the total number of sheets, and z_s and $\mathbf{v}_s$ are the instantaneous position of the sth plane and velocity of the sth beam particle).

The longitudinal component of the electric field is given by the Poisson equation $\partial E_z/\partial z=4\pi(\rho_b+\rho_p)$, with $\rho_p=e(n_0-n_p)$ and $\rho_p=-en_{\perp b}\Sigma_s\delta(z-z_s(t))$. The plasma is described by the cold nonrelativistic electron fluid equations:

$$\frac{\partial n_p}{\partial t}+\frac{\partial}{\partial z}(n_p u_{pz})=0, \tag{3}$$

$$\frac{\partial}{\partial t}\mathbf{u}_p+u_{pz}\frac{\partial}{\partial z}\mathbf{u}_p=-\frac{e}{m}\mathbf{E}-\frac{e}{mc}[\mathbf{u}_p\times(\mathbf{B}+\mathbf{B}_w)], \tag{4}$$

where $\mathbf{B}(\mathbf{B}_w)=\nabla\times\mathbf{A}(\mathbf{A}_w)$, $\mathbf{A}_w=a_w(\hat{\mathbf{e}}e^{-ik_wz}+\text{c.c.})/\sqrt{2}$ is the vector potential of the helical undulator magnetic field, $\hat{\mathbf{e}}=(\mathbf{e}_x+\mathbf{e}_y)/\sqrt{2}$, and $\mathbf{A}=A\hat{\mathbf{e}}+\text{c.c.}$ is the radiation vector potential. Furthermore, the equations for the beam electrons can be written as

$$\frac{dz_s(t)}{dt}=v_{\parallel s}(t), \tag{5}$$

$$\frac{dp_{\parallel s}(t)}{dt}=-\left\{\frac{e}{mc}E_z(z,t)+\frac{e^2c}{2m^2c^4\gamma_s}\frac{\partial}{\partial z}(\mathbf{A}+\mathbf{A}_w)^2\right\}_{z=z_S(t)}, \tag{6}$$

where $p_{\parallel s}=\beta_{\parallel s}\gamma_s$ and $\gamma_s=[1-v_s^2(t)/c^2]^{-1/2}$. Here the condition obtained from the transverse electron dynamics in the case of a purely axial injection of the beam, i.e., $\mathbf{p}_{\perp s}=(\mathbf{v}_{\perp s}/c)\gamma_s=(e/mc^2)(\mathbf{A}+\mathbf{A}_w)$, has been used.

We assume that the plasma, before the injection of the beam, is in a state of equilibrium without internal currents ($n_p=n_0$, $\mathbf{E}=\mathbf{0}$, $\mathbf{B}=\mathbf{0}$, $\mathbf{u}_p=\mathbf{0}$), and that the beam is so weak that it produces only small deviations from the equilibrium values.

Retaining only the linear terms and referring to the variables $\mathbf{E}_\perp=E_T\hat{\mathbf{e}}+\text{c.c.}$ and E_z, we obtain the following basic equations:

$$\left[\frac{\partial^2}{\partial t^2}-c^2\frac{\partial^2}{\partial z^2}+\omega_p^2\right]E_T=\frac{\omega_b^2a_w}{c\sqrt{2}}\frac{n_s}{n_{\perp b}}\frac{\partial}{\partial t}\sum_s\frac{1}{\gamma_s}e^{-ik_wz}\times\delta(z-z_s(t))-\frac{\omega_p^2}{c}u_{pz}(\mathbf{e}_z\times\mathbf{B}_w)\cdot\hat{\mathbf{e}}^*, \tag{7}$$

$$\left[\frac{\partial^2}{\partial t^2}+\omega_p^2\right]E_z=-4\pi\frac{\partial}{\partial t}J_{b,\parallel}-\frac{\omega_p^2}{c}(\mathbf{u}_{p\perp}\times\mathbf{B}_w)\cdot\mathbf{e}_z, \tag{8}$$

where $\omega_b^2=4\pi e^2n_b/m$. In the limit $\omega_c=eB_w/mc\ll\omega$ and when $n_b\ll n_p$, the dispersion relation of the system is very near to that of the cold nonmagnetized plasma, which comprises the two branches $\omega_L=\omega_p$ and $\omega=\sqrt{\omega_p^2+c^2k^2}$, the first branch being completely electrostatic, while the second has a purely transverse polarization. The electromagnetic branch is intersected by the beam resonance condition $\omega=(k+k_w)v_\parallel$ at two points, i.e., two values of k, and consequently of ω, satisfy this equation. These values of ω can be cast in the form given by Eq. (1), simply by redefining $X=\omega_p^2/(c^2k_w^2\beta_\parallel^2\gamma_\parallel^2)$.

The system given by the previous equations for the fields together with Eqs. (5) and (6) for the electrons, can be written in nondimensional form by introducing the definitions $\mathbf{E}_\perp=(1/c)(\partial\mathbf{A}/\partial t)$, $\mathbf{A}=A\hat{\mathbf{e}}+\text{c.c.}$, $A_T=eA/mc^2$, and the wiggler parameter $a_{w0}=ea_w/mc^2$ and can be substantially simplified by making use of the slowly varying envelope approximation, i.e., by putting $A_T=i(\tilde{A}_1e^{i(k_1z-\omega_1t)}+\tilde{A}_2e^{i(k_2z-\omega_2t)})$ and $n_p/n_0=A_Le^{i(k_Lz-\omega_Lt)}+\text{c.c.}$, with the hypothesis that $\tilde{A}_1$, $\tilde{A}_2$, and A_L are all slowly varying functions of time and space. Considering only the resonant terms, we obtain at last the equations

$$\left[\omega_1\frac{\partial}{\partial t}+c^2k_1\frac{\partial}{\partial z}\right]\tilde{A}_1=-\frac{\omega_b^2a_{w0}}{2\sqrt{2}}\left(\frac{n_{\perp b}}{n_b}\right)\sum_s\frac{1}{\gamma_s}e^{-i[k_wz_s+\phi_1(z_s)]}\times\delta(z-z_s(t)), \tag{9}$$

$$\left[\omega_2\frac{\partial}{\partial t}+c^2k_2\frac{\partial}{\partial z}\right]\tilde{A}_2=-\frac{\omega_b^2a_{w0}}{2\sqrt{2}}\left(\frac{n_{\perp b}}{n_b}\right)\sum_s\frac{1}{\gamma_s}e^{-i[k_wz_s+\phi_2(z_s)]}\times\delta(z-z_s(t)), \tag{10}$$

$$\left[\omega_L\frac{\partial}{\partial t}\right]A_L=-i\frac{\omega_b^2}{2}\left(\frac{n_{\perp b}}{n_b}\right)\sum_s e^{-i(k_Lz_s-\omega_Lt)}\delta(z-z_s(t)), \tag{11}$$

$$\frac{dz_z}{dt}=c\beta_{\parallel s}, \tag{12}$$

$$\frac{dp_s(t)}{dt}=\left\{\frac{i\omega_p^2}{ck_L}[e^{i\phi_L}A_L-\text{c.c.}]-\frac{ca_{w0}}{\sqrt{2}v_\parallel\gamma_s}\times[\omega_1\tilde{A}_1e^{i(\phi_1+k_wz)}+\omega_2\tilde{A}_2e^{i(\phi_2+k_wz)}+\text{c.c.}]\right\}_{z=z_S(t)}, \tag{13}$$

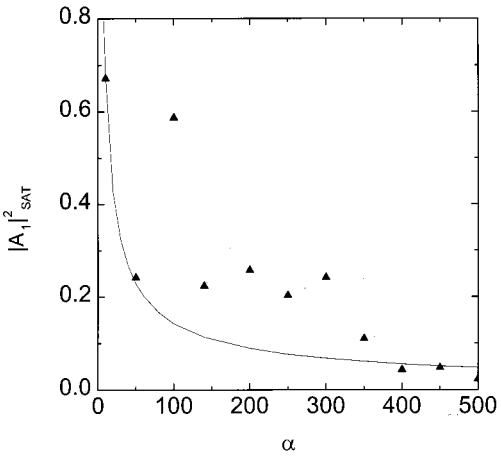

FIG. 1. Saturated signal $|A_1|^2_{\mathrm{SAT}}$ vs α for the excitation of the high-frequency wave ($\lambda_2=5\ \mu$m, $|A_2|=0.5$ at $\tau=0$). The solid curve gives a fit with $|A_1|^2_{\mathrm{SAT}}=a/\alpha^b$ ($a=3.27$, $b=0.68$) while the numerical results (solid triangles) show the existence of a more complicated structure for not very large values of α.

where $\phi_{1,2}=k_{1,2}z-\omega_{1,2}t$, $\phi_L=k_Lz-\omega_Lt$, $\gamma_s\cong\sqrt{1+a_{w0}^2+p_s^2(t)}$.

An analysis of the various electron phases in the momentum equation (13) shows that the two resonant electromagnetic waves do not give rise to any longitudinal mode, because ω_L is not coupled to the other two frequencies. We can therefore drop the electrostatic term in Eq. (13) which assumes the simpler form:

$$\frac{dp_s(t)}{dt}=-\left\{\frac{ca_{w0}}{\sqrt{2}v_{\parallel}\gamma_s}[\omega_1\tilde{A}_1e^{i(\phi_1+k_wz)}+\omega_2\tilde{A}_2e^{i(\phi_2+k_wz)}+\mathrm{c.c.}]\right\}_{z=z_S(t)}. \tag{14}$$

The coupling between the two electromagnetic waves is maintained because $k_1+k_w=\alpha(k_2+k_w)$, leading to the two phases being proportional for all values of time and space. If α is an integer, in particular, as the electrons of the beam are bunched on the long wavelength, they acquire a bunching also on the short wavelength, leading to a transfer of energy to the high-frequency wave. This system of equations has been integrated numerically along the characteristics, introducing the nondimensional variables $\tau=2ck_w\rho t$, $\zeta=2k_w\rho z$, and $A_{1,2}$, where ρ is the FEL parameter given by

$$\rho=\frac{1}{\gamma_0}\left(\frac{\omega_b^2a_{w0}^2}{16\beta_{\parallel}c^2k_w^2}\right)^{1/3}\quad\text{and}\quad A_{1,2}=i\frac{4\sqrt{2}ck_w\rho\gamma_0\omega_{1,2}}{\omega_b^2a_{w0}}\tilde{A}_{1,2}.$$

We assume that the long-wavelength wave acts as a pump wave and give a finite value to its amplitude $|A_2|$ at $\tau=0$. The other free parameters are a_{w0}, the initial energy of the beam (given by γ_0), α, ρ, and the length of the electron bunch L_b. The main effect of the pump is that of shortening decisively the lethargy time. The intensity of the signal obtained at saturation is, however, generally smaller than that generated spontaneously in a vacuum FEL.

In Fig. 1 we give the behavior of the signal intensity at saturation $|A_1|^2_{\mathrm{SAT}}$, as a function of α. The pump wavelength and strength are fixed at $\lambda_2=5\ \mu$m and $|A_2|=0.5$ (at $\tau=0$), while the beam injection energy is increasing from the value $\gamma_0=134$ when $\alpha=10$ ($\lambda_1=500$ nm, $\rho=9.2\times10^{-3}$), up to $\gamma_0=906$ when $\alpha=500$ ($\lambda_1=10$ nm, $\rho=1.4\times10^{-3}$). The other parameters have the values $n_0=4.4\times10^{16}$ cm^{-3}, $n_b=5.11\times10^{14}$ cm^{-3}, $a_{w0}=0.8$, $\lambda_w=1$ cm, $B_w=0.86$ T, and the bunch length $L_b=4$ mm. One can see that the efficiency of energy transfer to the upper resonant frequency is progressively decreasing with the increase in the frequency of the radiation excited with a rate that is approximately given by $|A_1|^2_{\mathrm{SAT}}\approx\alpha^{-0.68}$, for large values of α.

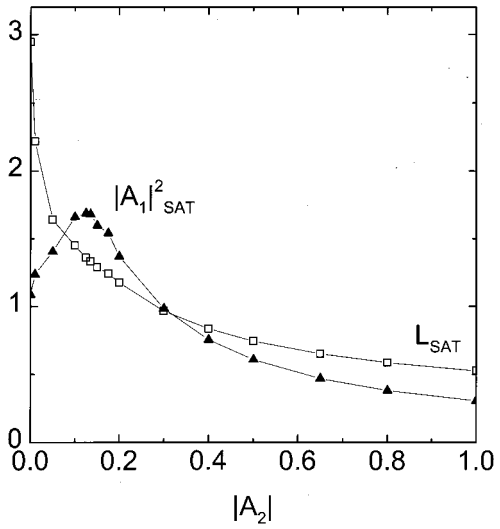

FIG. 2. Saturated signal $|A_1|^2_{\mathrm{SAT}}$ (solid triangles) and saturation length L_{SAT} in meters (hollow squares) vs the pump strength $|A_2|$ at $\tau=0$, for $\alpha=100$ and the signal wavelength $\lambda_1=50$ nm ($\lambda_2=5\ \mu$m). The usual vacuum SASE result for this case is $|A_1|^2_{\mathrm{SAT}}=1.25$ and $L_{\mathrm{SAT}}=3.1$ m.

Figure 2 shows the behavior of $|A_1|^2_{\mathrm{SAT}}$ and that of the saturation length L_{SAT} in meters vs the pump strength $|A_2|$ at $\tau=0$, all other parameters being kept fixed with the following values $\gamma_0=406.8$ (beam energy of 207.4 MeV at the injection), $\lambda_1=50$ nm, $\lambda_2=5\ \mu$m, $\alpha=100$, $\rho=3\times10^{-3}$, with n_0, n_b, B_w, and L_b as in Fig. 1. Figure 2 shows the reduction of the undulator length that is necessary in a plasma-loaded wiggler to reach signal saturation with the increase in the pump strength. The saturated signal intensity shows first a maximum at relatively low pump strengths, followed by a steady decrease with the scaling $|A_1|^2_{\mathrm{SAT}}\approx|A_2|^{-1}$. The values given in this figure can also be compared with those obtained in the usual one-dimensional FEL simulations, when there is no plasma and no account is taken of the low-frequency resonant wave. In the vacuum case, this last wave is counterpropagating with respect to the electron bunch and has no practical effects on the growth of the high-frequency wave. With the same values as before for γ_0, n_b, B_w, and L_b, one can show that, *in vacuum*, when there is no signal at $\tau=0$ and the FEL is operating in the self-amplified spontaneous emission (SASE) regime, $L_{\mathrm{SAT}}=3.1$ m and $|A_1|^2_{\mathrm{SAT}}=1.25$. From Fig. 2, one can see that the saturated values of the signal intensities that are obtained with the plasma loading and for rather low pump strengths

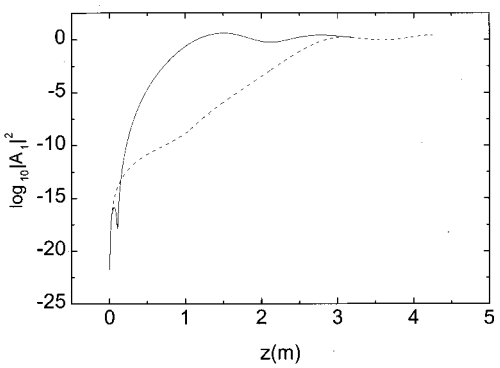

FIG. 3. $\log_{10}|A_1|^2$ vs the undulator length z in meters (solid curve), for the same case $\lambda_1=50$ nm with $|A_2|=0.1$ at $\tau=0$ ($N_T=2200$). The dashed curve shows the growth of the signal in the usual case in which the FEL is operating *in vacuum* and in the SASE regime.

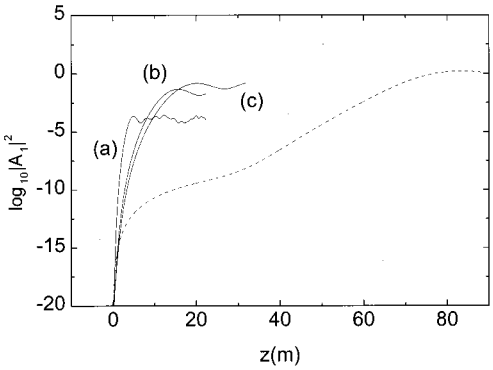

FIG. 4. $\log_{10}|A_1|^2$ vs the undulator length z(m), when $\lambda_1=1.5$ Å. The curves (a), (b), and (c) give the growth of the signal when the pump wave is, respectively, $|A_2|=10$, 1, and 0.6. The dashed curve shows the SASE growth without plasma.

($|A_2|<0.2$) even exceed the vacuum value (the maximum value in the case of Fig. 2 is $|A_1|^2_{\mathrm{SAT}}=1.6$ at $|A_2|\approx 0.15$).

Figure 3 gives the actual profile of $|A_1|^2$ vs the distance z in meters along the undulator, compared with the growth in the usual vacuum and SASE regime, for the same parameters as before, with the pump strength $|A_2|=0.1$. The beam bunching factor at the higher frequency $b_1=(1/N_T)\Sigma_j e^{-i[\phi_1 k_w z_j(t)]}$ has the value $|b_1|=4.6\times 10^{-4}$ at $\tau=0$ in both cases. All numerical results confirm that with the low-frequency pump and the plasma-loaded undulator the radiation emitted at the first maximum, i.e., at saturation, follows the same scaling laws as the usual SASE single-passage radiation.

In Fig. 4 we give, as a last example, a case in the x-ray region, in which the excited wave has the wavelength $\lambda_1=1.5$ Å. In this case, we use parameters whose values are near to the values assumed in the LCLS project [7], in which the FEL is operating in single pass, and the signal is starting from noise. We have chosen $\gamma_0=28\,700$ (beam energy 14.66 GeV), the wiggler period is $\lambda_w=3$ cm, $\rho=3\times 10^{-4}$, $\alpha=4000$ ($\lambda_2=0.6$ μm), $a_{w0}=2.69$ corresponding to a peak value of the magnetic field of the helical undulator $B_w=0.96$ T and the beam length is $L_b=4$ mm. As in Fig. 3, we compare the usual vacuum growth of the signal, which has a saturation length of about 85 m and a saturated intensity $|A_1|^2_{\mathrm{SAT}}=0.92$, with the signal increase in the plasma-loaded case and with three values of the pump wave at $\tau=0$, namely, $|A_2|=10$, 1, and 0.6. With the first value of the pump strength, i.e., $|A_2|=10$, the signal saturates at $L_{\mathrm{SAT}}\approx 5$ m, with $|A_1|^2_{\mathrm{SAT}}=0.025$, while $L_{\mathrm{SAT}}=15.6$ m and $|A_1|^2_{\mathrm{SAT}}=0.23$ and $L_{\mathrm{SAT}}=20$ m and $|A_1|^2_{\mathrm{SAT}}=0.8$, when the pump is at the values 1 and 0.6, respectively. One can see that the present scheme could be used as a convenient alternative method of reducing the great length of the undulator as proposed in this project, and of controlling, at the same time, the intensity of the x-ray output radiation pulse.

[1] N. Piovella, V. Petrillo, C. Maroli, and R. Bonifacio, Phys. Rev. Lett. **72**, 88 (1994).

[2] E. J. Sternbach and H. Ghalila, Nucl. Instrum. Methods Phys. Res. A **304**, 691 (1991).

[3] Y.-H. Liu and T. C. Marshall, Nucl. Instrum. Methods Phys. Res. A **375**, 589 (1996); Phys. Rev. E **56**, 2161 (1997).

[4] T. Lefevre, J. Gardelle, G. Marchese, J. L. Rullier, and J. T. Donohue, Phys. Rev. Lett. **82**, 323 (1999).

[5] J. B. Murphy, C. Pellegrini, and R. Bonifacio, Opt. Commun. **53**, 197 (1985).

[6] Xiaojian Shu, Phys. Rev. E **55**, 3489 (1997).

[7] The LCLS Design Study Group, Stanford Linear Accelerator Center (SLAC) Report No. SLAC-R-521, 1998 (unpublished).